Spinodal electronic phase separation during insulator-metal transitions

Yin Shi*
Department of Materials Sciences and Engineering, Pennsylvania State University, University Park, Pennsylvania 16802, USA

Long-Qing Chen†
Department of Materials Sciences and Engineering, Materials Research Institute, Department of Engineering Science and Mechanics, and Department of Mathematics, Pennsylvania State University, University Park, Pennsylvania 16802, USA

(Received 15 May 2020; revised 19 October 2020; accepted 20 October 2020; published 2 November 2020; corrected 4 June 2021)

Electronic phase transitions such as insulator-metal transitions are common in strongly correlated systems. Here, using a combination of thermodynamic linear-stability analysis and phase-field simulations and employing VO_2 as a prototypical example, we predict that an insulator-metal transition driven by photoexcitation may involve an intermediate, modulated charge density state with a temperature-dependent characteristic wavelength. It is shown that such an intermediate two-phase electronic state is formed through a spinodal mechanism and that its formation can be generic for insulator-metal transitions driven by fast stimuli. This transient electronic phase separation is expected to stimulate future experimental and computational efforts.

DOI: 10.1103/PhysRevB.102.195101

I. INTRODUCTION

Spinodal phase separation, which occurs when a homogeneous state becomes thermodynamically unstable with respect to phase separation to two or more phases, is ubiquitous in nature. For example, a homogeneous liquid separates into a liquid-vapor two-phase mixture when it becomes mechanically unstable, i.e., the isothermal compressibility becomes negative [1]. A homogeneous binary solution decomposes into two phases with different chemical compositions when its chemical instability is reached or the second derivative of its free energy with respect to the chemical composition becomes negative [2]. Recently, it was shown that the ferroelastic domain structure formation at a constant strain often takes place through the spinodal mechanism due to the thermodynamic instability of the parent phase with respect to mechanical strain [3]. Commercial porous glasses with interconnected nanometer-scale pores, with a wide variety of applications such as chromatography, reference electrodes, catalysis support, etc., are typically obtained through the spinodal phase separation mechanism.

For complex materials, a homogeneous state at low temperatures is generally unstable with respect to the development of different types of order such as charge/spin/lattice order and phase separation, leading to competing ground states with distinct electronic properties [4–7]. Some of these states may coexist on microscopic and mesoscopic length scales, e.g., the coexistence of metallic and insulating states responsible for the colossal magnetoresistance [8,9]. Here, using vanadium dioxide (VO_2) as an example, we report the observation of an *intermediate* electronic phase separation through a spinodal mechanism during the insulator-metal transition (IMT) driven by ultrafast photoexcitation in our phase-field simulations, and our analytical thermodynamic analysis demonstrates that such an electronic phase separation results from the instability of a transient homogeneous state against the development of charge density modulations with a characteristic wavelength.

VO_2 is perhaps the most studied material that undergoes an IMT at a temperature $T_c = 340$ K under ambient pressure accompanied by a change in the lattice structure [10,11]. Below T_c, VO_2 is an insulator with a monoclinic structure, called the M1 phase, while above T_c it is a metal with a rutile structure, labeled the R phase [10–12]. To describe the coupled electronic and structural phase transition, we recently proposed a thermodynamic description employing two sets of order parameters: One is a multicomponent electronic order parameter characterizing the electronic transition, and the other is a multicomponent structural order parameter describing the structural transition, which are also coupled to the spatially inhomogeneous distributions of charge carriers, namely the free electrons and holes [13–15].

II. MINIMAL MESOSCOPIC MODEL OF IMT

Before we perform phase-field simulations to explore the possible spinodal electronic phase separation in VO_2 upon photoexcitation, we start with a minimal mesoscopic model to analyze and understand the possible emergence of transient insulator-metal coexistence states of a crystal going through a generic insulator-metal transition. Here, we utilize a single spatially dependent order parameter field $\xi(\boldsymbol{r}, t)$, where $\boldsymbol{r} = (x, y, z)$ represents the spatial coordinate and t is the time, to present a metallic state ($\xi = 0$), or an insulating state ($\xi \neq 0$, with $\pm\xi$ describing two energetically degenerate insulating state or domain variants), or a mixture of metallic and insulating regions within a crystal. The thermodynamics of such

*yxs187@psu.edu
†lqc3@psu.edu

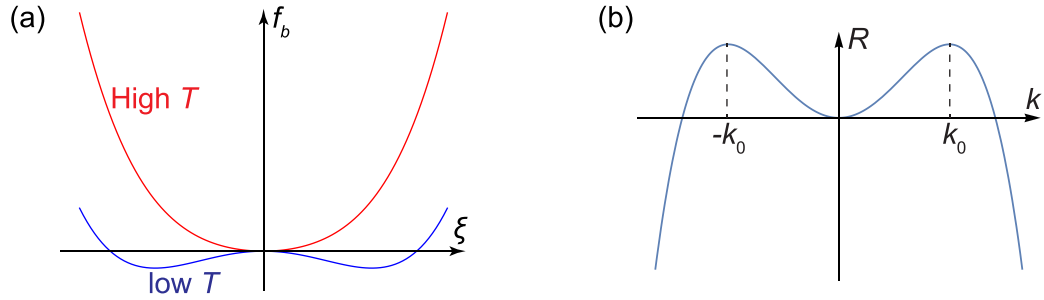

FIG. 1. (a) A schematic intrinsic bulk free-energy density f_b as a function of order parameter ξ at different temperatures, and (b) a schematic amplification factor R as a function of the wave number k. In (a), at high temperatures f_b has a minimum at $\xi = 0$ corresponding to the metallic phase, while at low temperatures it has two degenerate minima at nonzero $\pm\xi$ corresponding to two energetically degenerate states of the insulating phase.

an inhomogeneous system can be described by the following simplest possible free-energy functional,

$$F = \int \left[f(T;\xi,n,p) + \frac{\kappa}{2}(\nabla\xi)^2 \right] d^3r, \tag{1}$$

where f is the local free energy density, T is temperature, $n(\boldsymbol{r},t)$ and $p(\boldsymbol{r},t)$ are the free electron and hole density fields, respectively, and κ is the gradient energy coefficient. The system is assumed to be at partial equilibrium within local degrees of freedom of ξ, n, and p, respectively, so that it has well-defined local T and ξ as well as n and p that obey equilibrium statistical distributions with their own quasichemical potentials. Without loss of generality, we employ the following simple model for f,

$$f = f_b(T;\xi) + k_BT\left\{ n\ln\frac{n}{N_c} + p\ln\frac{p}{N_v} + 2n_i + \left[\frac{E_g(\xi)}{2k_BT} - 1\right](n+p)\right\}. \tag{2}$$

Here, $f_b(T;\xi)$ is the intrinsic bulk free energy density [see Fig. 1(a)], and the second term is the relative free energy density of the free charge carriers under the Boltzmann statistics approximation [14,15]. N_c and N_v are the effective electronic densities of states at the conduction and valence band edges of the insulating state, respectively. $n_i = \sqrt{N_cN_v}\exp[-E_g(\xi)/2k_BT]$ is the intrinsic electron concentration in the insulating state.

In Eq. (2), E_g is the electron energy gap, which depends on the order parameter ξ, that is, there is a finite gap in the insulating state $\xi \neq 0$, and the gap is closed in the metallic state $\xi = 0$. Since E_g is a scalar invariant degenerate with respect to $\pm\xi$ insulating states, the lowest-order, symmetry-allowed expansion for E_g is $E_g = \gamma\xi^2$, where γ is a positive constant.

A. Linear-stability analysis

To analyze the temporal and spatial evolution of the charge carriers, we assume that the charge neutrality $n = p$ is satisfied everywhere, and the possible carrier recombination can be ignored regarding the short timescale of the process of concern. We also assume that the IMT takes place much faster than the diffusion process of the free charge carriers, i.e., ξ is at equilibrium for a given distribution of n at any moment. In one dimension, the equilibrium of ξ at a given spatial distribution of n is achieved by minimizing the functional F with respect to ξ,

$$\frac{\partial f_b}{\partial\xi} - \kappa\frac{\partial^2\xi}{\partial x^2} + 2\gamma\xi(n-n_i) = 0. \tag{3}$$

The diffusion equation for n is

$$\frac{\partial n}{\partial t} = \frac{\partial}{\partial x}\left(\frac{Mn}{e}\frac{\partial}{\partial x}\frac{\delta F}{\delta n}\right) = \frac{M}{e}\left\{\gamma\left[\xi\frac{\partial\xi}{\partial x}\frac{\partial n}{\partial x} + n\left(\frac{\partial\xi}{\partial x}\right)^2 + n\xi\frac{\partial^2\xi}{\partial x^2}\right] + k_BT\frac{\partial^2 n}{\partial x^2}\right\}, \tag{4}$$

where M is the mobility of the free electrons, and e is the (positive) elementary charge, and $\delta F/\delta n$ represents the variational derivative of F with respect to n, i.e., the quasichemical potential of the free electrons.

We can write n as a function of ξ from Eq. (3) and then substitute it into Eq. (4) to obtain a differential equation of ξ only. We now examine the stability of a homogeneous state, described by a uniform ξ, against infinitesimal fluctuations in ξ, i.e., we consider a solution with a uniform value $\bar{\xi}$ plus an infinitesimal modulation with a wave number k,

$$\xi = \bar{\xi} + A_k(t)\exp(ikx), \tag{5}$$

where $A_k(t)$ is an infinitesimal amplitude. Introducing an infinitesimal modulation in ξ also produces an infinitesimal modulation in the electron (hole) density. Substituting Eq. (5) into Eqs. (3) and (4) gives, to the first order of $A_k(t)$,

$$\frac{dA_k(t)}{dt} = R(k)A_k(t), \tag{6}$$

and its solution is simply $A_k(t) = \exp[R(k)t]$, where $R(k)$ is the amplification factor,

$$R(k) = -\frac{M}{e}\frac{h_1k^2 + h_2k^4}{h_3 + h_4k^2}. \tag{7}$$

Here,

$$h_1 = \frac{k_BT}{\gamma}\frac{\partial^2 f_b}{\partial\xi^2}\bigg|_{\bar{\xi}} + \left(\bar{\xi} - \frac{k_BT}{\gamma\bar{\xi}}\right)\frac{\partial f_b}{\partial\xi}\bigg|_{\bar{\xi}}, \tag{8a}$$

$$h_2 = \frac{k_BT\kappa}{\gamma}, \tag{8b}$$

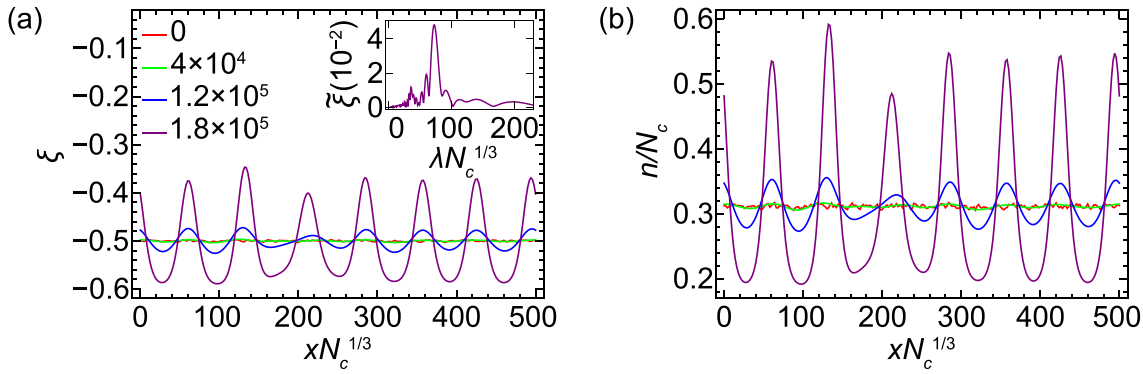

FIG. 2. (a) and (b) show the temporal evolution of ξ and n, respectively, during electronic phase separation during an IMT. The legend in (a) lists the times in units of $e/Mk_BT_0N_c^{2/3}$. The inset in (a) is the Fourier transform of ξ at $t = 1.8 \times 10^5 e/Mk_BT_0N_c^{2/3}$ (λ is the wavelength).

$$h_3 = \frac{2\gamma\bar{\xi}^2\bar{n}_i}{k_BT} + \frac{1}{\gamma}\left(\left.\frac{\partial^2 f_b}{\partial\xi^2}\right|_{\bar{\xi}} - \frac{1}{\bar{\xi}}\left.\frac{\partial f_b}{\partial\xi}\right|_{\bar{\xi}}\right), \tag{8c}$$

$$h_4 = \frac{\kappa}{\gamma}, \tag{8d}$$

where $\bar{n}_i = \sqrt{N_cN_v}\exp(-\gamma\bar{\xi}^2/2k_BT)$.

For small k, we can expand $R(k)$ to the fourth order of k,

$$R(k) \approx -\frac{M}{e}\left(\frac{h_1}{h_3}k^2 + \frac{h_2h_3 - h_1h_4}{h_3^2}k^4\right). \tag{9}$$

If $h_1/h_3 > 0$ and $h_2h_3 - h_1h_4 > 0$, $R(k)$ in Eq. (9) is always negative, implying that the initial homogeneous state is stable. The equilibrium case $(\partial f_b/\partial\xi)|_{\bar{\xi}} = 0$, $(\partial^2 f_b/\partial\xi^2)|_{\bar{\xi}} > 0$ is indeed in the stable regime. On the other hand, for $h_1/h_3 < 0$ and $h_2h_3 - h_1h_4 > 0$, or equivalently,

$$\frac{1}{\bar{\xi}}\left.\frac{\partial f_b}{\partial\xi}\right|_{\bar{\xi}} - \frac{2\gamma^2\bar{\xi}^2\bar{n}_i}{k_BT} < \left.\frac{\partial^2 f_b}{\partial\xi^2}\right|_{\bar{\xi}} < \left(1 - \frac{\gamma\bar{\xi}^2}{k_BT}\right)\frac{1}{\bar{\xi}}\left.\frac{\partial f_b}{\partial\xi}\right|_{\bar{\xi}}, \tag{10}$$

$R(k)$ in Eq. (9) as a function of k is shown in Fig. 1(b). A $\bar{\xi}$ satisfying inequalities (10) describes a nonequilibrium state. As it can be seen, the system is unstable for a range of k, i.e., those k yielding $R(k) > 0$,

$$|k| < \sqrt{\frac{-h_1h_3}{h_2h_3 - h_1h_4}}, \quad k \neq 0. \tag{11}$$

$R(k)$ has two positive maxima at $\pm k_0$, with $k_0 = \sqrt{-h_1h_3/2(h_2h_3 - h_1h_4)}$. Since $A_k(t)$ grows exponentially with time with $R(k)$, the dominant A_k's are those at and around $k = \pm k_0$, leading to a modulation of ξ with a characteristic wavelength

$$\lambda_0 = \frac{2\pi}{k_0} = 2\pi\sqrt{\frac{2(h_2h_3 - h_1h_4)}{-h_1h_3}}. \tag{12}$$

Therefore, for a $\bar{\xi}$ satisfying inequalities (10), the initial nonequilibrium homogeneous phase with order parameter $\bar{\xi}$ will spontaneously separate into a mixture of a metal-like phase and an insulatorlike phase.

B. Numerical solution

To confirm the above linear-stability analysis, we numerically solve Eqs. (3) and (4) with periodic boundary conditions for both ξ and n. We use a simple double-well potential for f_b, $f_b = -4f_0(\tau\xi^2/2 + \xi^4/4)$ with $\tau = (T - T_0)/T_0$, which describes a second-order phase transition at a critical temperature T_0. f_0 is the equilibrium free energy density at $T = 0$ K. We choose the following parameters for numerical calculations: $f_0 = -0.25k_BT_0N_c$, $\kappa = 8k_BT_0N_c^{1/3}$, and $\gamma = 5k_BT_0$.

The result for temperature $\tau = -0.5$ is shown in Fig. 2. The initial ξ is assigned a uniform nonequilibrium value $\bar{\xi} = -0.5$ plus an uncorrelated random noise ranging from -0.005 to 0.005, which is inside the unstable regime defined by inequalities (10). Indeed, the noise grows with time with a dominant wavelength, which is shown clearly in the Fourier transform of ξ ($\tilde{\xi}$) at $t = 1.8 \times 10^5 e/Mk_BT_0N_c^{2/3}$. The highest peak in $\tilde{\xi}$ is at the wavelength $\lambda_0 = 74N_c^{-1/3}$, which is very close to the $\lambda_0 = 72N_c^{-1/3}$ estimated using Eq. (12). We also observed the expected coarsening of the metal-like phase (peaks of ξ) and the insulatorlike phase (valleys of ξ) at later stages (not shown). If a sink term representing the electron-hole recombination process (the process for n to approach n_i) were introduced, we would have seen the eventual evolution of the transient insulator-metal mixture to the equilibrium homogeneous insulator with $\xi = -\sqrt{-\tau} = -1/\sqrt{2}$. The simulation of the cases inside the stable regime shows that the initial noises gradually disappear and that the system directly evolves to the equilibrium homogeneous insulating state. It should be pointed out that in the conventional chemical spinodal decomposition in binary solutions, solute-concentration modulations with finite wavelengths arise from the competition between the reduction in the bulk chemical energy and the gradient energy [2] whereas the transient electronic phase separation results from the coupling between the electronic order parameter and the charge carriers [Eqs. (3) and (4)].

III. TRANSIENT ELECTRONIC PHASE SEPARATION IN PHOTOEXCITED VO_2

We next discuss the transient electronic phase separation of nonequilibrium states that resulted during the photoinduced IMT in VO_2.

A. Phase-field model of IMT in photoexcited VO_2

We shall follow our earlier work on the phase-field model of VO_2 [13–15]. The structural and the electronic phases in VO_2 can be characterized by a set of structural order parameters $\{\eta_i,\ i=1,2,3,4\}$ and a set of electronic order parameters $\{\xi_i,\ i=1,2,3,4\}$, respectively [13–15]. A finite η_i indicates the dimerization of the neighboring V ions, and a finite ξ_i indicates the formation of the dynamical singlet situated on the neighboring V sites and consequently the opening of the energy gap [16–18]. The order parameters of the different phases are $\eta_1=\eta_3\neq 0$, $\eta_2=\eta_4=0$, $\xi_1=\xi_3\neq 0$, $\xi_2=\xi_4=0$, $\eta_1\xi_1<0$, $\eta_3\xi_3<0$ (and other symmetry-related values) for the M1 phase and $\eta_i=\xi_i=0$ $(i=1,2,3,4)$ for the R phase [13]. Since only the R and the M1 phases are involved and since no multidomain structure is present, we simplify the problem by reducing the two sets of the four-dimensional order parameters to two one-dimensional order parameters, $\eta=(\eta_1+\eta_3)/\sqrt{2}$ and $\xi=(\xi_1+\xi_3)/\sqrt{2}$ (here, $\eta_2=\eta_4=\xi_2=\xi_4=0$ always).

The Landau free-energy functional of VO_2 is written as

$$\begin{aligned}&F_{\mathrm{VO_2}}[T,\Phi(\boldsymbol{r},t);\eta(\boldsymbol{r},t),\xi(\boldsymbol{r},t),n(\boldsymbol{r},t),p(\boldsymbol{r},t)]\\&\quad=F_0^{\mathrm{VO_2}}[T;\eta(\boldsymbol{r},t),\xi(\boldsymbol{r},t)]\\&\qquad+F_f^{\mathrm{VO_2}}[T,\Phi(\boldsymbol{r},t);\xi(\boldsymbol{r},t),n(\boldsymbol{r},t),p(\boldsymbol{r},t)],\end{aligned}\tag{13}$$

where $F_0^{\mathrm{VO_2}}$ and $F_f^{\mathrm{VO_2}}$ are the intrinsic free energy and the free energy of free electrons and holes, respectively, and Φ is the electric potential. $F_0^{\mathrm{VO_2}}$ consists of a bulk Landau potential $f_b^{\mathrm{VO_2}}$ and a gradient energy punishing the spatial variance of the order parameters, $F_0^{\mathrm{VO_2}}=\int[f_b^{\mathrm{VO_2}}+\kappa_1(\nabla\eta)^2/2+\kappa_2(\nabla\xi)^2/2]d^3r$, where κ_1 and κ_2 are positive constants. The bulk Landau potential reads [13–15]

$$\begin{aligned}f_b^{\mathrm{VO_2}}=&\frac{a_1(T-T_1)}{2T_c}\eta^2+\frac{b_1}{4}\eta^4+\frac{c_1}{6}\eta^6\\&+\frac{a_2(T-T_2)}{2T_c}\xi^2+\frac{b_2}{4}\xi^4+\frac{c_2}{6}\xi^6\\&+h\eta\xi-\frac{s}{2}\eta^2\xi^2+\frac{q}{2}\eta^3\xi,\end{aligned}\tag{14}$$

where a_1, a_2, b_1, b_2, c_1, c_2, h, s, q, T_1, and T_2 are all constants. The free energy of free electrons and holes in VO_2 is calculated based on the assumption that the conduction and the valence bands are effectively parabolic [15],

$$\begin{aligned}F_f^{\mathrm{VO_2}}=\int\Bigg[&\frac{E_g(\xi)}{2}(n+p)+k_BT\int_0^n F_{1/2}^{-1}\left(\frac{\zeta}{N_c}\right)d\zeta\\&+k_BT\int_0^p F_{1/2}^{-1}\left(\frac{\zeta}{N_v}\right)d\zeta+e\Phi(p-n)\Bigg]d^3r-F_i^{\mathrm{VO_2}},\end{aligned}\tag{15}$$

where $F_{1/2}^{-1}$ is the inverse function of the Fermi integral $F_{1/2}(u)=(2/\sqrt{\pi})\int_0^\infty\sqrt{\epsilon}[1+\exp(\epsilon-u)]^{-1}d\epsilon$ [19] and $F_i^{\mathrm{VO_2}}$ is the equilibrium intrinsic free energy of free electrons and holes serving as a reference energy. The effective density of states of the conduction (valence) band $N_{c(v)}$ is related to the effective mass of the free electrons (holes) $m^*_{e(h)}$, $N_{c(v)}=2(m^*_{e(h)}k_BT/2\pi\hbar^2)^{3/2}$. The energy gap is related to the electronic order parameter ξ [16–18] to its symmetry-allowed lowest order, $E_g=\gamma\xi^2$ [13–15], where γ is a constant fitted to the experimentally measured gap.

The mesoscale kinetics of the phase transitions in VO_2 upon photoexcitation is described by the Ginzburg-Landau equations for η and ξ and the diffusion equations for n and p,

$$\frac{\partial\eta(\boldsymbol{r},t)}{\partial t}=-L_1\frac{\delta F_{\mathrm{VO_2}}}{\delta\eta(\boldsymbol{r},t)},\tag{16}$$

$$\frac{\partial\xi(\boldsymbol{r},t)}{\partial t}=-L_2\frac{\delta F_{\mathrm{VO_2}}}{\delta\xi(\boldsymbol{r},t)},\tag{17}$$

$$\frac{\partial n(\boldsymbol{r},t)}{\partial t}=\nabla\cdot\left[\frac{M_e n(\boldsymbol{r},t)}{e}\nabla\frac{\delta F_{\mathrm{VO_2}}}{\delta n(\boldsymbol{r},t)}\right]+\Gamma(\boldsymbol{r},t),\tag{18}$$

$$\frac{\partial p(\boldsymbol{r},t)}{\partial t}=\nabla\cdot\left[\frac{M_h p(\boldsymbol{r},t)}{e}\nabla\frac{\delta F_{\mathrm{VO_2}}}{\delta p(\boldsymbol{r},t)}\right]+\Gamma(\boldsymbol{r},t),\tag{19}$$

which are closed by the Poisson equation for the self-consistent determination of the electric potential $\Phi(\boldsymbol{r},t)$,

$$-\nabla^2\Phi(\boldsymbol{r},t)=\frac{e[p(\boldsymbol{r},t)-n(\boldsymbol{r},t)]}{\epsilon_r\epsilon_0}.\tag{20}$$

Here, $\Gamma(\boldsymbol{r},t)$ represents the rate per unit volume of photoexcitation of free electron-hole pairs. L_1 and L_2 are constants characterizing the phase transition speed, and $M_{e(h)}$ is the electron (hole) mobility. ϵ_r and ϵ_0 are the relative permittivity of VO_2 and the vacuum permittivity, respectively. The electron-hole recombination process can be ignored here since the lifetime of free electrons and holes in VO_2 ($\sim$10 μs [20]) is found to be much longer than the timescale of the transient electronic phase separation.

For a monochrome light linearly polarized along the x direction (propagating in the z direction) with an angular frequency ω and an intensity I, Γ can be derived from the Fermi's golden rule,

$$\begin{aligned}\Gamma=&\frac{2\pi}{\hbar V}\sum_{\boldsymbol{k}_i,\boldsymbol{k}_f}[1-f_F(\epsilon_{c\boldsymbol{k}_f}-\mu_e)]\left|\frac{e\tilde{A}}{m}p_{fi}\right|^2 f_F\left(\epsilon_{v\boldsymbol{k}_i}+\mu_h\right)\\&\times\delta\left(\epsilon_{c\boldsymbol{k}_f}-\epsilon_{v\boldsymbol{k}_i}-\hbar\omega\right),\end{aligned}\tag{21}$$

where m is the electron mass, $\hbar$ is the Planck constant divided by 2π, $f_F(\varepsilon)=[1+\exp(\varepsilon/k_BT)]^{-1}$ is the Fermi distribution function, $\tilde{A}$ is the amplitude of the vector potential of the light, V is the illuminated volume, and $p_{fi}=\langle c\boldsymbol{k}_f|p_x|v\boldsymbol{k}_i\rangle$ is the momentum matrix element connecting the $\boldsymbol{k}_i$ state in the valence band and the $\boldsymbol{k}_f$ state in the conduction band. For a general polarization, the vector potential of the light can be written as $\tilde{A}\boldsymbol{n}$ where the complex vector $\boldsymbol{n}$ is the polarization direction. Then the momentum matrix element appearing in the modulus operator in Eq. (21) is $\boldsymbol{n}\cdot\boldsymbol{p}_{fi}$, where $\boldsymbol{p}_{fi}=(\langle c\boldsymbol{k}_f|p_x|v\boldsymbol{k}_i\rangle,\langle c\boldsymbol{k}_f|p_y|v\boldsymbol{k}_i\rangle)$. In such a general case, one needs to explicitly calculate $\boldsymbol{p}_{fi}$ including the phase factors of its components, which requires the detail of the electronic structure of the material and is beyond the scope of the present mesoscopic continuous theory. The momentum of the photon has been ignored since it is negligible compared to the momentum of the electron. $\epsilon_{v\boldsymbol{k}}=-\hbar^2k^2/2m^*_h-E_g/2$ and $\epsilon_{c\boldsymbol{k}}=\hbar^2k^2/2m^*_e+E_g/2$ are the energy spectra of the

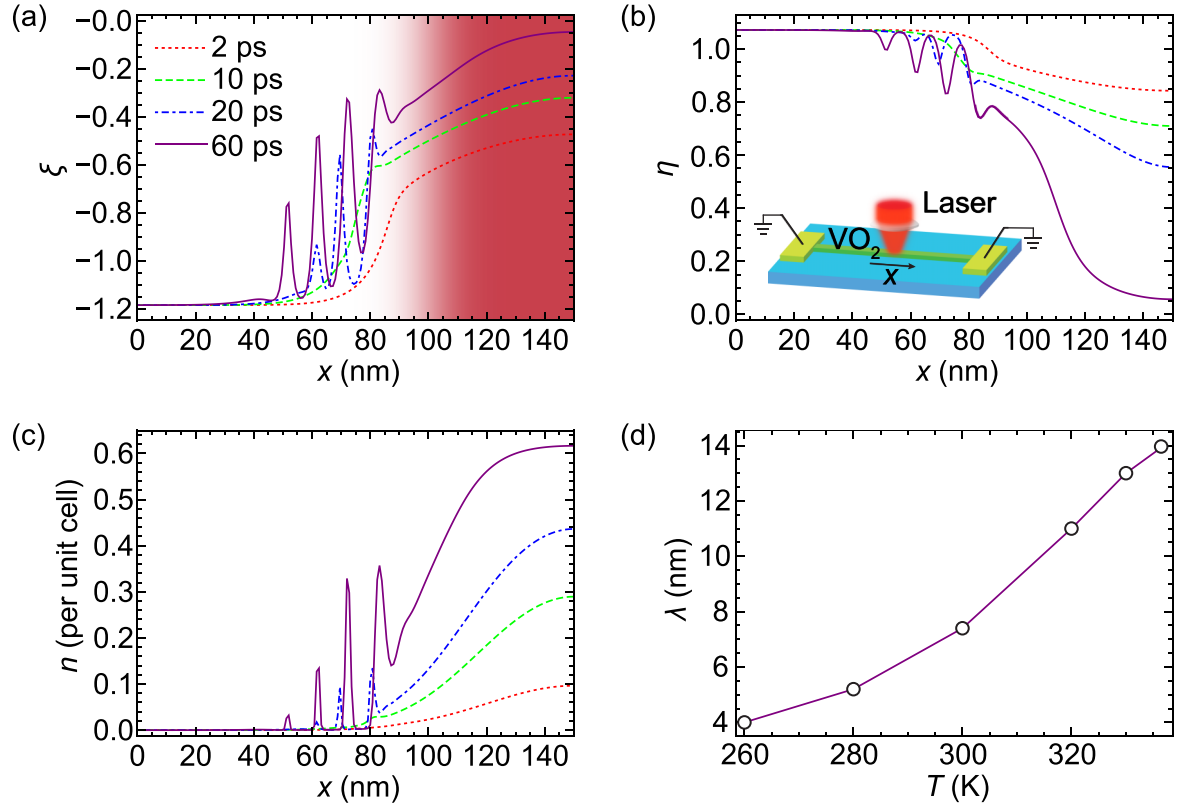

FIG. 3. Phase-field simulation results on the transient electronic phase separation in a 300-nm-long VO_2 nanobeam at $T = 320$ K photoexcited by an 800-nm laser pulse of 2 mJ/cm^2 fluence and 0.2 ns duration. (a)–(c) depict the temporal evolution of ξ, η, and n, respectively. p is almost the same as n. The inset in (b) is a schematic of the simulation setup. We only show the results on half of the sample ($0 \leqslant x \leqslant 150$ nm) [the shaded region in (a) indicates the half of the illuminated region]. The results on the other half are symmetrical with the shown results about the $x = 150$ nm mirror plane. (d) Dominant wavelength of the phase modulation as a function of temperature in the photoexcited VO_2. The line is a guide to the eyes.

parabolic valence and conduction bands, respectively. Since the effective mass of holes in VO_2 has not been measured, we adopt a rough approximation that $m_h^* = m_e^*$ [20]. μ_e and μ_h are the quasichemical potentials of free electrons and free holes, respectively. Note that the quasichemical potential of the valence electrons is the negative quasichemical potential of the holes μ_h here. For the two-parabolic-band model, the momentum matrix element can be approximated from the $\boldsymbol{k} \cdot \boldsymbol{p}$ perturbation theory $|p_{fi}|^2 \approx \delta_{\boldsymbol{k}_f \boldsymbol{k}_i}(1 + m/m_h^*)mE_g/2$ [21]. $\tilde{A}$ is related to the intensity I by $I = \epsilon_0 c\omega^2 \tilde{A}^2/2$, where c is the speed of light in the vacuum. Using these relations and doing the summation in Eq. (21), we have

$$\Gamma = \frac{\sqrt{2\pi N_v N_c} e^2 E_g I}{\epsilon_0 cm\omega^2 \hbar k_B T}\left(1 + \frac{m}{m_h^*}\right)\sqrt{\frac{\hbar\omega - E_g}{k_B T}} \times f_F\left(-\frac{\hbar\omega}{2} + \mu_h\right)\left[1 - f_F\left(\frac{\hbar\omega}{2} - \mu_e\right)\right], \quad (22)$$

in which we have used $m_e^* = m_h^*$ so that $N_v = N_c = \sqrt{N_c N_v}$.

I is a Gaussian-type function of both the space and the time controlling the illumination range and duration of the pump laser pulse: In the one-dimensional case $I(x,t) = \sqrt{e} I_0 g_\delta(x - x_0) g_\zeta(t - t_0)$, where $g_\sigma(\epsilon) = \exp(-\epsilon^2/2\sigma^2)$ and I_0 is defined as the intensity of the laser pulse. The illumination width and the pulse duration are defined as 4δ and 2ζ, respectively. x_0 and t_0 are the position and the moment of the peak of the laser pulse, respectively.

B. Photoinduced transient electronic phase separation

We consider a VO_2 nanobeam (one-dimensional system) with its middle part illuminated by a 800-nm laser pulse and its two ends connected to the ground [inset in Fig. 3(b)]. The corresponding boundary conditions are that the electric potential Φ is zero, and that n and p have their equilibrium values at the two ends. We assume Neumann boundary conditions (zero spatial derivatives) for η and ξ, which is the manifestation of no interaction of the order parameters with the environment. The parameters of the light used in the simulation are $I_0 = 10^7$ W/cm^2, $\delta = 25$ nm, $x_0 = 150$ nm, $\zeta = 0.1$ ns, and $t_0 = 0.2$ ns, corresponding to a $2I_0\zeta = 2$ mJ/cm^2 fluence and $2\zeta = 0.2$ ns duration laser pulse. The period of the 800-nm laser is 2.67 fs, which is far shorter than the scattering time 18.5 fs estimated from the electron mobility of 0.5 cm^2/V s [22].

Figure 3 presents the results for VO_2 upon photoexcitation. Inside the illuminated region, the photoexcitation produces free electron-hole pairs, which screen the electron-electron repulsion and thus the electron correlation described by the electronic order parameter [23]. This eventually leads to the closure of the energy gap resulting in the transition from the insulator to the metal inside the illuminated region,

which is consistent with the femtosecond time-resolved photoelectron spectroscopy measurement and the first-principles many-body perturbation theory calculations [23]. The IMT inside the illuminated region is accompanied by the diffusion of the excited free electrons and holes outside the illuminated region and the formation of a nonequilibrium electronic state there. As it can be seen clearly, charge density modulation with a wavelength of ∼11 nm forms at the edge of the illuminated region (around $x \sim 70$ nm) several picoseconds following the incidence of the laser, inducing the coexistence of metal-like (high carrier density) and insulatorlike (low carrier density) phases. A wavelike ionic displacement field (represented by the structural order parameter η) also develops at the edge of the illuminated region due to the coupling between the electronic and the structural order parameters. The metal-like and the insulatorlike phases also undergo coarsening at later stages.

We calculate the characteristic wavelength of the phase modulation at different temperatures, as shown in Fig. 3(d). The wavelength increases with elevating temperature and reaches the maximum of ∼14 nm near T_c. The wavelengths are far shorter than the diffusion length of the free carriers (several micrometers [20]). At low temperatures the modulation wavelength may be calculated to be subnanometers, implying the possibility of charge ordering at the atomic scale.

IV. CONCLUSIONS AND DISCUSSIONS

We formulated the theory and computational model for studying coupled electronic and structural phase transitions under fast stimuli. We demonstrated both analytically and computationally that an IMT driven by ultrafast stimuli is likely preceded by a transient electronic phase separation of the excited nonequilibrium electronic states into charge density modulations with a dominant wavelength. This work is expected to stimulate future experimental investigations to detect and explore the transient electronic phase separation phenomena and the modulated states of charge density and ionic displacement fields in VO_2 and related materials that exhibit IMTs.

In the phase-field model of VO_2, we made the approximation of parabolic bands for both the conduction and the valence bands, while the band structure of VO_2 is much more complicated than this approximation [24,25]. The complicated band structure will result in a complicated diffusion equation. Although the exact time and spatial scales of the electronic phase separation will definitely depend on the details of the band structure, we argue that our conclusion for the existence of the phase separation is insensitive to the details of the band structure. Our argument is based on the fact that the important factors for the possible emergence of the phase separation are the spontaneous change in the band gap and a natural gradient energy of the order parameter responsible for the possible domain wall energy. This is demonstrated by the emergence of the phase separation in both our minimal model and the actual VO_2 model despite the difference in the details of the diffusion equations in the two models.

We also assumed the hole effective mass to be the same as the electron effective mass. The effective mass of holes in VO_2 is expected to be different from that of electrons due to the asymmetric conduction and valence bands. Nevertheless, this may just have a minor influence on the results. Since the mobilities of the free electrons and the free holes in VO_2 are close to each other [20], the charge neutrality is expected to be approximately fulfilled everywhere in the system during the phase separation, as demonstrated in our simulation. Hence, only the diffusion equation and consequently the effective mass of the free electrons are important. The different effective mass of the free holes affects the rate of the photoexcitation of free electron-hole pairs, but it has a minimal influence on the phase separation because the phase separation does not occur inside the illuminated region and the important consequence of the photoexcitation is the formation of a nonequilibrium state at the edges of the illuminated region. Therefore, the timescale and wavelength of the phase separation should be insensitive to the different effective mass of free holes.

ACKNOWLEDGMENTS

The initial stage of the work was supported by the Penn State MRSEC, Center for Nanoscale Science, under Award No. NSF DMR-1420620, and the late stage of this work was supported as part of the Computational Materials Sciences Program funded by the U.S. Department of Energy, Office of Science, Basic Energy Sciences, under Award No. DE-SC0020145.

[1] L. Landau and E. Lifshitz, *Statistical Physics, Part 1: Volume 5*, 3rd ed. (Butterworth-Heinemann, Oxford, UK, 1980).
[2] J. W. Cahn, Acta Metall. **9**, 795 (1961).
[3] F. Xue, Y. Li, Y. Gu, J. Zhang, and L.-Q. Chen, Phys. Rev. B **94**, 220101(R) (2016).
[4] S.-W. Cheong, P. Sharma, N. Hur, Y. Horibe, and C. Chen, Phys. B: Condens. Matter **318**, 39 (2002).
[5] A. Moreo, S. Yunoki, and E. Dagotto, Science **283**, 2034 (1999).
[6] S. Yunoki, J. Hu, A. L. Malvezzi, A. Moreo, N. Furukawa, and E. Dagotto, Phys. Rev. Lett. **80**, 845 (1998).
[7] E. Dagotto, S. Yunoki, A. L. Malvezzi, A. Moreo, J. Hu, S. Capponi, D. Poilblanc, and N. Furukawa, Phys. Rev. B **58**, 6414 (1998).
[8] M. Uehara, S. Mori, C. Chen, and S.-W. Cheong, Nature (London) **399**, 560 (1999).
[9] E. Dagotto, T. Hotta, and A. Moreo, Phys. Rep. **344**, 1 (2001).
[10] F. J. Morin, Phys. Rev. Lett. **3**, 34 (1959).
[11] A. Zylbersztejn and N. F. Mott, Phys. Rev. B **11**, 4383 (1975).
[12] J. H. Park, J. M. Coy, T. S. Kasirga, C. Huang, Z. Fei, S. Hunter, and D. H. Cobden, Nature (London) **500**, 431 (2013).
[13] Y. Shi, F. Xue, and L.-Q. Chen, Europhys. Lett. **120**, 46003 (2017).
[14] Y. Shi and L.-Q. Chen, Phys. Rev. Materials **2**, 053803 (2018).
[15] Y. Shi and L.-Q. Chen, Phys. Rev. Applied **11**, 014059 (2019).
[16] S. Biermann, A. Poteryaev, A. I. Lichtenstein, and A. Georges, Phys. Rev. Lett. **94**, 026404 (2005).

[17] H. Zheng and L. K. Wagner, Phys. Rev. Lett. **114**, 176401 (2015).
[18] W. H. Brito, M. C. O. Aguiar, K. Haule, and G. Kotliar, Phys. Rev. Lett. **117**, 056402 (2016).
[19] A. N. Morozovska, E. A. Eliseev, O. V. Varenyk, Y. Kim, E. Strelcov, A. Tselev, N. V. Morozovsky, and S. V. Kalinin, J. Appl. Phys. **116**, 066808 (2014).
[20] C. Miller, M. Triplett, J. Lammatao, J. Suh, D. Fu, J. Wu, and D. Yu, Phys. Rev. B **85**, 085111 (2012).
[21] P. Y. Yu and M. Cardona, *Fundamentals of Semiconductors: Physics and Materials Properties*, 4th ed. (Springer, Berlin, 2010).
[22] W. H. Rosevear and W. Paul, Phys. Rev. B **7**, 2109 (1973).
[23] D. Wegkamp, M. Herzog, L. Xian, M. Gatti, P. Cudazzo, C. L. McGahan, R. E. Marvel, R. F. Haglund, A. Rubio, M. Wolf, and J. Stähler, Phys. Rev. Lett. **113**, 216401 (2014).
[24] M. Gatti, F. Bruneval, V. Olevano, and L. Reining, Phys. Rev. Lett. **99**, 266402 (2007).
[25] C. Weber, S. Acharya, B. Cunningham, M. Grüning, L. Zhang, H. Zhao, Y. Tan, Y. Zhang, C. Zhang, K. Liu, M. Van Schilfgaarde, and M. Shalaby, Phys. Rev. Res. **2**, 023076 (2020).

Correction: The omission of a support statement in the Acknowledgments has been fixed.